Exploratory modelling of the impacts of sea-level rise on the Sundarbans mangrove forest, West Bengal, India

Sourav Samanta[1], Sugata Hazra[1*], Jon R. French[2], Robert J Nicholls[3], Partho P. Mondal[1]

[1]School of Oceanographic Studies, Jadavpur University, 188 Raja S. C. Mullick Road, Kolkata 700032, West Bengal, India; ssamanta.sos.rs@jadavpuruniversity.in (SS); sugata.hazra@jadavpuruniversity.in* (SH); partho.iirs@gmail.com (PPM)

[2]Coastal and Estuarine Research Unit, UCL Department of Geography, University College London, London WC1E 6BT, UK; j.french@ucl.ac.uk (JRF)

[3]Tyndall Centre for Climate Change Research, University of East Anglia, Norwich NR4 7TJ, UK (RJN); Robert.Nicholls@uea.ac.uk

[*]Correspondence: sugata.hazra@jadavpuruniversity.in

Abstract

In this paper we conduct exploratory simulations of the possible evolution of the Indian Sundarbans mangroves to 2100 under a range of future sea-level rise (SLR) scenarios, considering the effects of both inundation and shoreline erosion. The Sea Level Affecting Marshes Model (SLAMM) is used to simulate habitat transitions due to inundation and these outputs are combined with an empirical model of SLR-driven shoreline erosion. A set of plausible climate-induced SLR scenarios are considered, together with delta subsidence and constrained vertical sediment accretion. Significant mangrove decline is found in all cases: the greater the rise in sea level the greater the losses. By the end of the century, the Indian Sundarbans mangroves could lose between 42 % and 80 % of their current area if current management is continued. Managed realignment could offset these losses but at the expense of productive land and the migration of the human population.

Keywords: SLAMM; Sundarbans; Climate Change; Coastal Erosion; Sea Level Rise

Graphical abstract

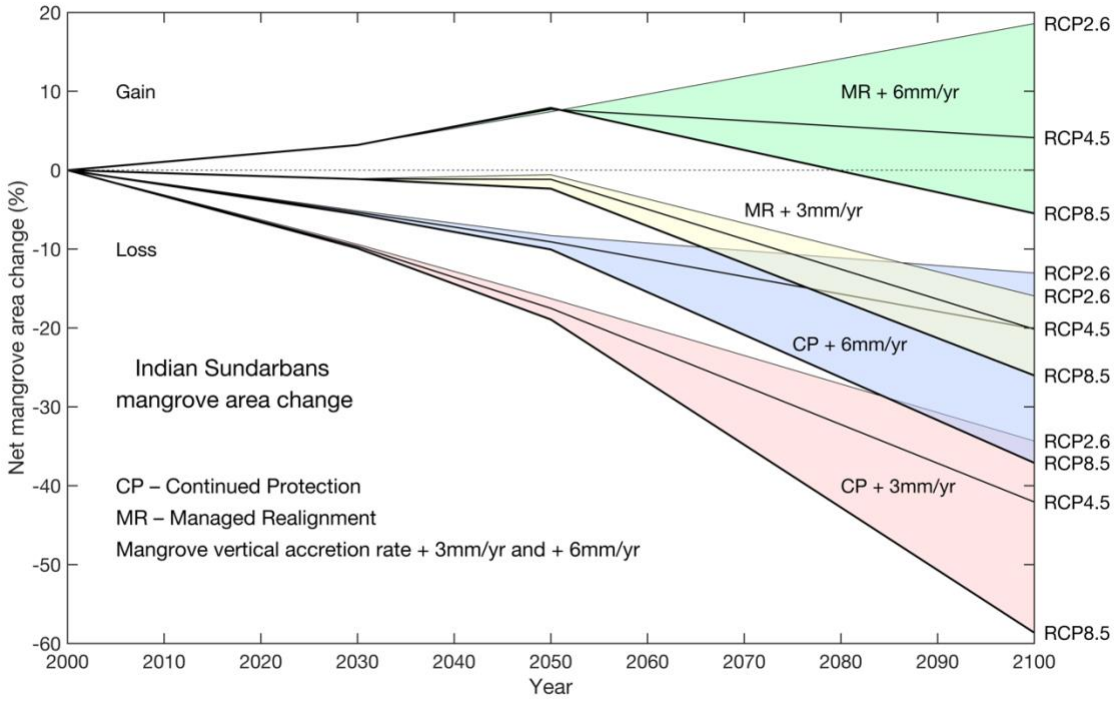

1. Introduction

Mangroves are one of the most productive ecosystems on Earth (Sriyanie, 2008; Carugati et al., 2018) and provide vital ecosystem services, including raw materials and food, protection against coastal erosion and storm surge inundation, water purification, maintenance of fisheries, carbon sequestration, and tourism/recreation (Barbier et al., 2011). All coastal ecosystems are potentially vulnerable to sustained sea-level rise (SLR) (Nicholls and Cazenave, 2010), and this may be exacerbated by other aspects of climate change and human-induced stresses. In the case of mangroves, SLR can drive loss by submergence, where vertical sedimentation is insufficient to maintain surface elevations (Woodroffe et al., 2016; Saintilian et al., 2020), as well as by increased rates of shoreline erosion and retreat (Wu et al. 2015). Spencer et al. (2016) projected the loss of up to 78% of the world's coastal wetlands by 2100 under a high (1.1 m) SLR scenario, although Schuerch et al. (2018) noted that such losses might be significantly reduced or even avoided where accommodation space allows landward migration. Alongi (2008) projected that 10 to 15% of mangrove forest will be lost by 2100 due to climate-driven SLR. Regionally, Gilman et al. (2006) predicted a 13% decline of mangrove forest in the Pacific islands by 2100. Loss of mangroves degrades all the associated ecosystem services identified above, with multiple adverse impacts. Of particular importance is the loss of natural protection against storm surges (Menéndez et al., 2020).

All these vulnerabilities are evident in the Sundarbans, which covers about 10,000 km^2, and is the world's largest contiguous mangrove forest (Sarker et al., 2016). Stretching between India and Bangladesh, the Sundarbans is rich in biodiversity and is the main habitat of the critically endangered Royal Bengal Tiger. Most SLR impact assessments to date have considered the Bangladesh Sundarbans and have projected quite varied outcomes. Huq et al. (1995) estimated that the Bangladesh Sundarbans would be completely inundated and lost under a 1.0 m SLR, while Loucks et al. (2010) predicted that most parts would be inundated for a SLR of 0.28 m using 2000 as a base year. Mukul et al. (2019) predicted that the entire Bangladesh Sundarbans will be submerged by 2070 due to the combined effect of climate change and sea-level rise. In contrast to these rather pessimistic findings, Lovelock et al. (2015) argued that the Sundarbans mangroves could survive a much more rapid SLR scenario (1.48 m by 2100). Similarly, Payo et al. (2016) projected only around 10% loss in the mangrove area of Bangladesh Sundarbans by 2100 under the same 1.48 m SLR scenario. Given the local, regional and global importance of the Sundarbans,

these contrasting results demonstrate a need for further analyses to better understand likely future changes and their management implications.

In the past few years, various models have been developed to quantify the impacts of SLR on coastal habitats and thereby support better management of these environments. For example, there have been extensive bespoke modelling efforts in the Mississippi delta (Costanza et al., 1990; Reyes et al., 2000; White et al., 2019), although these approaches are difficult to transfer to other locations due to their high data requirements. More generalised models have also been developed that, although limited in their ability to represent many of the underlying geomorphological and ecological processes in detail, are useful for exploratory analyses. Of these, the Sea Level Affecting Marshes Model (SLAMM) has found wide application in varied wetland environments around the world (e.g. Akumu et al., 2011; Li et al., 2015; Payo et al., 2016; Tabak et al., 2016; Cole Eckberg et al., 2017; Prado et al., 2019). SLAMM simulates the dominant factors influencing coastal wetland habitat type at broad spatial and temporal scales (Craft et al., 2009; McLeod et al., 2010; Clough et al., 2016) and the habitat transitions that occur in response to SLR. SLAMM has already been used in the Sundarbans of Bangladesh (Payo et al., 2016), based upon the assumption of static inundation and a constant rate of shoreline erosion. Their results suggested that erosion is the dominant driver of land loss for low rates of SLR (up to 0.5 m/century), with inundation becoming the dominant process under mid- to high-range SLR scenarios (more than 0.5 m/century). However, they did not include the effects of increased vertical sediment accretion as sea level rises, and their use of a constant shoreline erosion rate in SLAMM neglects the non-linear land loss under time-varying SLR that is known to be an important process in this region (Samanta et al., 2021). No such modelling has yet been undertaken for the Indian Sundarbans, and it is clear that some refinement of the basic SLAMM model is needed if the simulated changes in mangrove location and extent are to be plausible.

The aim of this study is to simulate indicative habitat transitions in the Indian Sundarbans, including mangrove loss and migration, under a range of 21st century climate change scenarios. This aim is delivered through the implementation of a novel hybrid model that combines SLAMM simulation of inundation-driven habitat change with an empirical model of SLR-driven shoreline erosion. A series of exploratory simulations are performed using the RCP2.6, RCP4.5, and RCP8.5 climate change scenarios for global SLR, with additional consideration of geological subsidence in the delta region and a constraint on the ability of the mangroves to accrete vertically. The hybrid

SLAMM model is also used to illustrate the potential implications of a major managed realignment to allow inland northwards mangrove migration, including its effects on human activities.

2. Study Area

The Indian Sundarbans was declared as the Sundarban Biosphere Reserve (SBR) in 1989 under the United Nations Educational Scientific and Cultural Organization (UNESCO) Man and Biosphere (MAB) Reserve Programme. The Indian SBR (21° 32′ N–22° 40′ N and 88° 05′ N–89° 51′ E) covers an area of 9,630 km^2 (https://en.unesco.org/biosphere/aspac/sunderban), including more than 4,200 km^2 of protected mangrove forests (including creek, estuary and forest) in 2020 of which approximately 1,880 km^2 is actual forest cover (Samanta et al. 2021). Mangroves extend across the border into the Bangladesh Sundarbans, collectively forming the largest contiguous mangrove forest on earth. The Sundarbans evolved with the formation and evolution of the Ganges–Brahmaputra River delta over the Holocene (Stanley and Hait, 2000; Allison et al., 2003) and comprise numerous low islands and mudflats separated by anastomosing fluvial and tidal channels. The SBR can be divided into core, buffer, and transition zones (Figure 1). In the core area, no human activities are permitted. The buffer zone is uninhabited, but fishing and related activities are permitted. Both comprise continuous mangroves. In contrast, the transition zone is densely populated with intensive agricultural land use and other economic activities (Marcinko et al., 2021). There are more than 1000 villages in 19 Community Development Blocks (CDBs) within the South 24 Parganas (13 Blocks) and the North 24 Parganas (6 blocks) districts of West Bengal, and a total population of 4.4 million (Census, 2011; Table S2 in Supplementary Materials). The rapidly expanding adjacent megacity of Kolkata exerts a significant influence on the demographic and economic trends of the SBR.

The main estuaries in the SBR are funnel-shaped and orientated north to south. They are interconnected by a complex network of east-to-west channels. The tidal range is between 3.5 and 4 m, with a strong lunar 18.6-year nodal cycle (Pitchaikani, 2020). Tide gauges show an upward trend in relative sea level, which includes the effect of long-term geological subsidence of the delta plain (Hazra et al., 2002; Brown and Nicholls, 2015). Much of the transition zone of the SBR lies below normal tidal levels and is protected from regular flooding by dikes and polders. Landfall of

tropical cyclones and the associated surges originating in the Bay of Bengal are recurring hazards, causing wind damage and floods, especially when dikes fail (Ali et al., 2020). The region is characterized by a tropical climate with a dry season between November and April and a wet monsoonal period over the rest of the year. Annual precipitation is between 1500 and 2000 mm. Seasonal mean minimum and maximum temperatures vary from 12°C to 24°C and 25°C to 35°C, respectively (Padhy et al., 2020).

The Sundarban mangroves belong floristically to the Indo-Andaman mangrove province within the species-rich Indo-West Pacific group (Ghosh et al., 2015). Twenty-four true mangrove taxa from nine different families are present (Barik and Chowdhury, 2014). There is a land to sea and east to west zonation within the Sundarbans mangroves across India and Bangladesh. This reflects variation in relative SLR, salinity and sediment input. Relative SLR varies due to tectonic uplift in the west and subsidence in the east. There is more monsoonal freshwater and sediment input to the eastern and western parts, resulting in more saline conditions in the central part (where the ground is also higher) (Barik et al., 2018; Rahman et al., 2022). Historically, there has been significant encroachment and reclamation into the mangroves for human use, especially agriculture. Although the Indian Sundarbans mangroves are now protected from direct human destruction, mangrove area declined by 110 km^2 (5.5 km^2 $year^{-1}$) from 2000 to 2020, reflecting both erosion and submergence (Samanta et al., 2021). Similar losses have been seen in the Bangladesh Sundarbans (Giri et al., 2007).

3. Methods

3.1 SLAMM overview

SLAMM version 6.7 (Warren Pinnacle Consulting, 2016) was chosen on account of its simplicity and minimal data requirements, while acknowledging its limited physical basis. SLAMM was first developed in the mid-1980s to simulate coastal habitat transitions and associated land loss due to SLR at broad spatial scales. It is essentially a kinematic model that neglects any constraint imposed by a sediment budget and simply considers the balance between inundation and vertical accretion in each cell of a raster digital elevation model (DEM). A decision tree allows transitions to occur between habitat types, for example, if the elevation of a cell declines below a minimum required elevation for the existing habitat in that cell. Vertical accretion can be specified as a constant rate,

or as a non-linear function of the cell elevation within the tidal frame (Clough et al., 2010, Li et al., 2015). Selected DEM cells can be masked to represent dry land or land that is protected from inundation by dikes. Land loss due to erosion can also be simulated for both fetch-limited and open coastal situations using algorithms of varying sophistication, depending on the availability of bathymetric and wind climate data and observational erosion data for calibration.

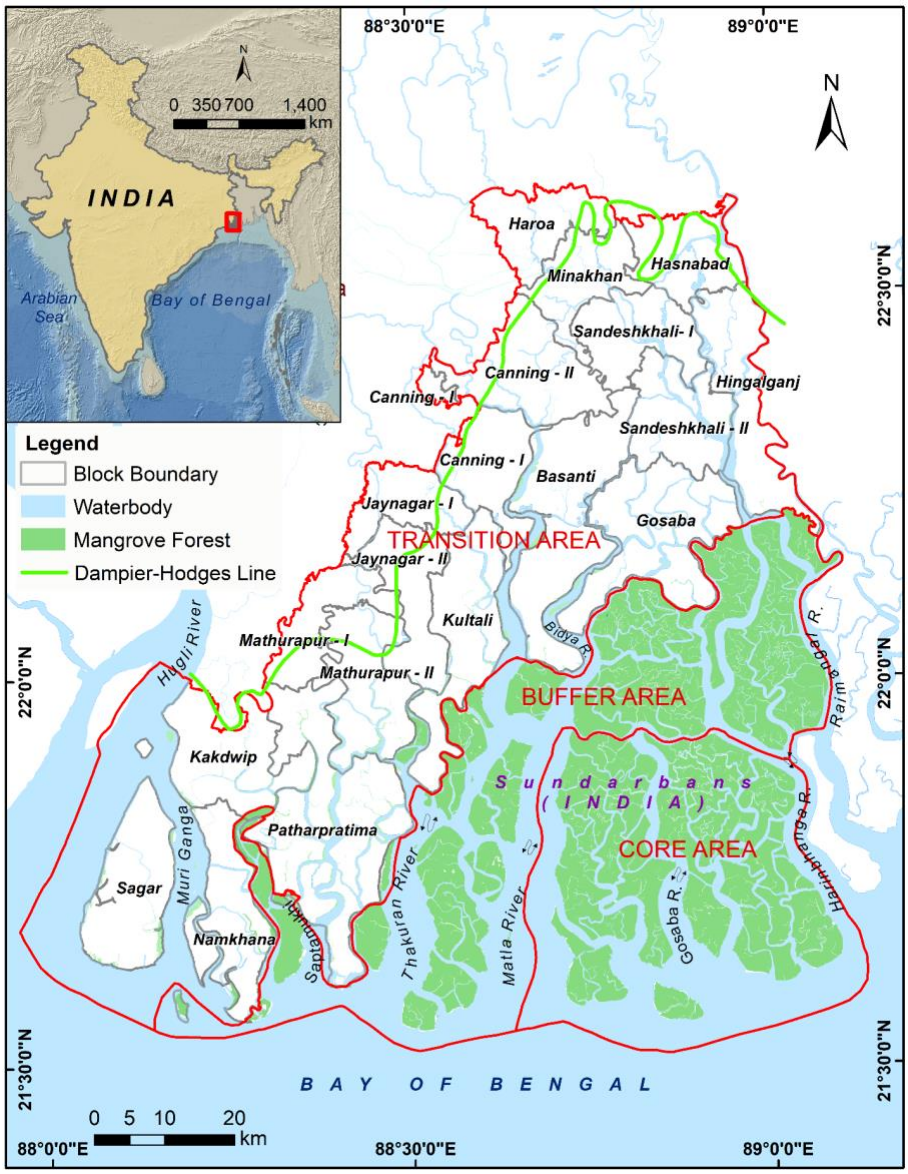

Figure 1. Location map showing the Indian Sundarbans and the three management zones. The Dampier-Hodges line was mapped in 1829-1830 and still marks the approximate landward limit of mangrove and estuarine tidal influence.

The principal model inputs are a DEM of suitable accuracy and spatial resolution and a set of similarly dimensioned raster layers describing the topographic slope, land cover and wetland habitat class. Wetland habitats are defined using the US National Wetlands Inventory (NWI) classification, which is developed for North America and requires some adjustment for application in the Sundarbans region (see below). SLAMM also requires specification of the vertical tidal frame in terms of a Great Diurnal Tide Range (GDTR), and parameter values for the selected accretion and erosion sub-models.

3.2 Raster input layers

3.2.1 DEM and slope

A DEM with high vertical accuracy and spatial resolution is required to achieve meaningful results in SLAMM. Lidar data are not presently available for the Sundarbans, and therefore, a range of satellite-derived DEM products (SRTM (Farr et al., 2007), TanDEM (Rizzoli et al., 2017), CoastalDEM (Kulp and Strauss, 2018) were evaluated. These were compared to a ground surveyed DEM constructed from point-based elevation data (2276 points) acquired on Mousuni Island, West Bengal, using a micro-optic theodolite on a 100 x 100 m grid. Elevations were referenced to a Survey of India permanent benchmark at the former Collectorate building in the centre part of the island and GPS was used to determine the point locations. For comparison with the satellite-derived products, the surveyed DEM was interpolated to a resolution of 90 x 90 m using inverse distance weighting. CoastalDEM showed the best agreement to the survey elevation data (Figure 2) and was selected for the SLAMM analysis. The spatial resolution of CoastalDEM is 3 arc seconds (~90 m) and its vertical uncertainty is estimated as < 1 m. Figure 3a,b shows the resulting DEM and a derived topographic slope raster layer generated using the slope tool in ArcGIS 10.5.

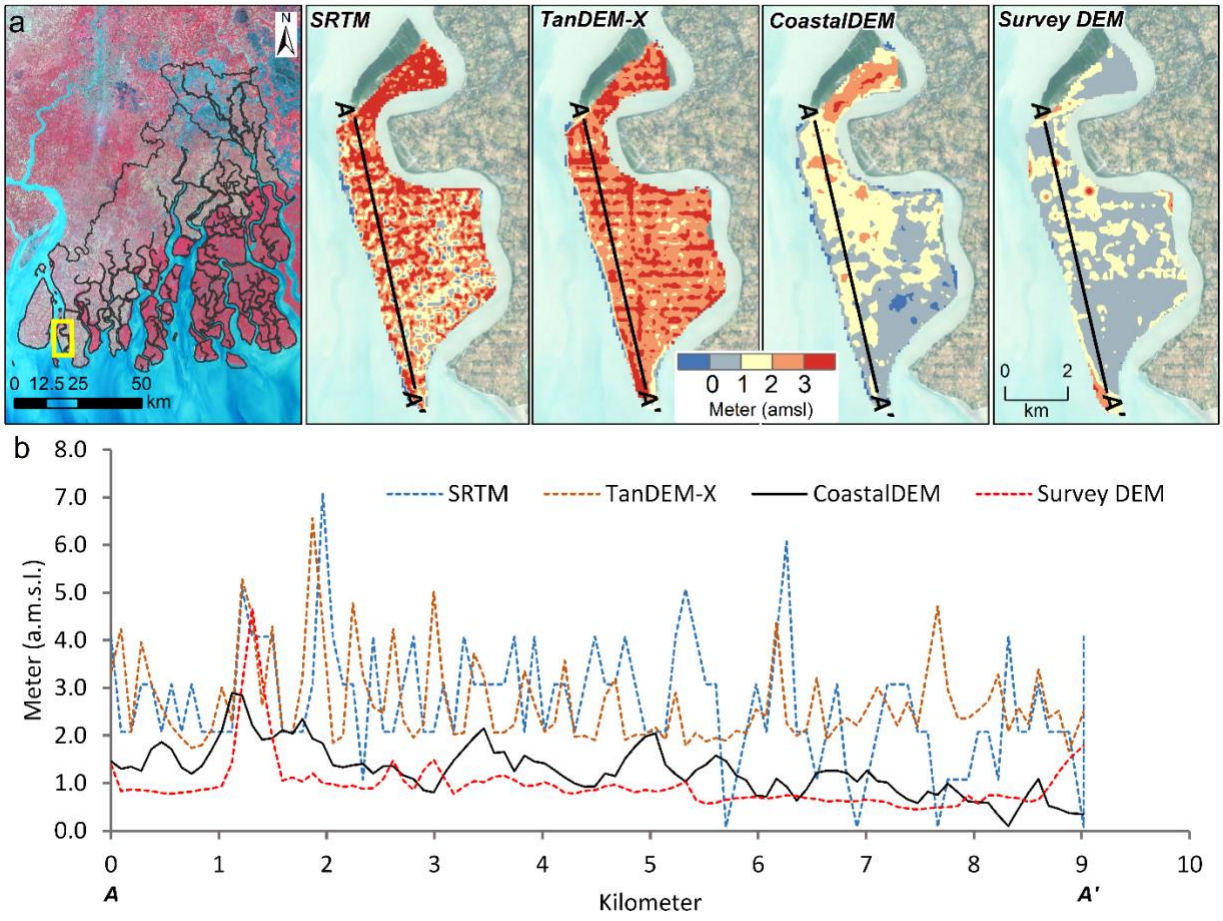

Figure 2. Comparison between ground surveyed elevations and the CoastalDEM, SRTM and TanDEM products at Mousuni Island: a) map showing location of survey transect; b) comparison of surveyed and DEM product elevations along transect A-A`

3.2.2 Wetland habitat layer

A land use/land cover (LULC) map was generated (Figure 3d) using Landsat-TM data from 2001. The US NWI classification is embedded within the SLAMM 6.7 program code and this is not directly applicable to the range of habitats found in the Sundarbans. Accordingly, LULC classes were adjusted to use the nearest NWI classes. For example, the 'urban settlement' class was assigned to 'developed dry land', rural settlement-crop and-barren land was assigned to undeveloped dry land, Aquaculture was assigned to transitional salt marsh, saline blank to

regularly flooded marsh, water bodies to inland open water, and river and creek was represented by estuarine open water.

3.2.3 Subsidence layer

Stanley and Hait (2000) estimated a maximum subsidence of 5.0 mm yr^{-1} in the Indian Sundarbans based on geological evidence. Brown and Nicholls (2015) conducted a more systematic review of land subsidence rates across the Ganges–Brahmaputra–Meghna delta, using 205 data points derived using a range of methods and timescales. The Sundarbans showed the lowest mean (2.8 mm yr^{-1}) and median (2.0 mm yr^{-1}) rates of net subsidence compared with other land uses in the delta. Payo et al. (2016) used a net subsidence rate of 2.5 mm yr^{-1} in their SLAMM simulations of the Bangladesh Sundarbans and made the reasonable assumption that subsidence is linear over short geological (decadal to centennial) timescales. In the present study we similarly use a uniform subsidence rate of 2.5 mm yr^{-1} for the entire SBR and assume that this is constant to 2100.

3.2.4 Flood defence (dike) layer

The location of dikes and polders are key to understand where mangroves can or cannot exist. A flood defence (dike) layer (Figure 3c) was generated by on-screen digitization in Google Earth. The resulting KML file was converted to a raster of the same dimensions as all the other inputs. An arbitrary crest elevation of 5 m was assigned to all dike pixels to ensure that protected areas remained dry for all the SLR scenarios considered.

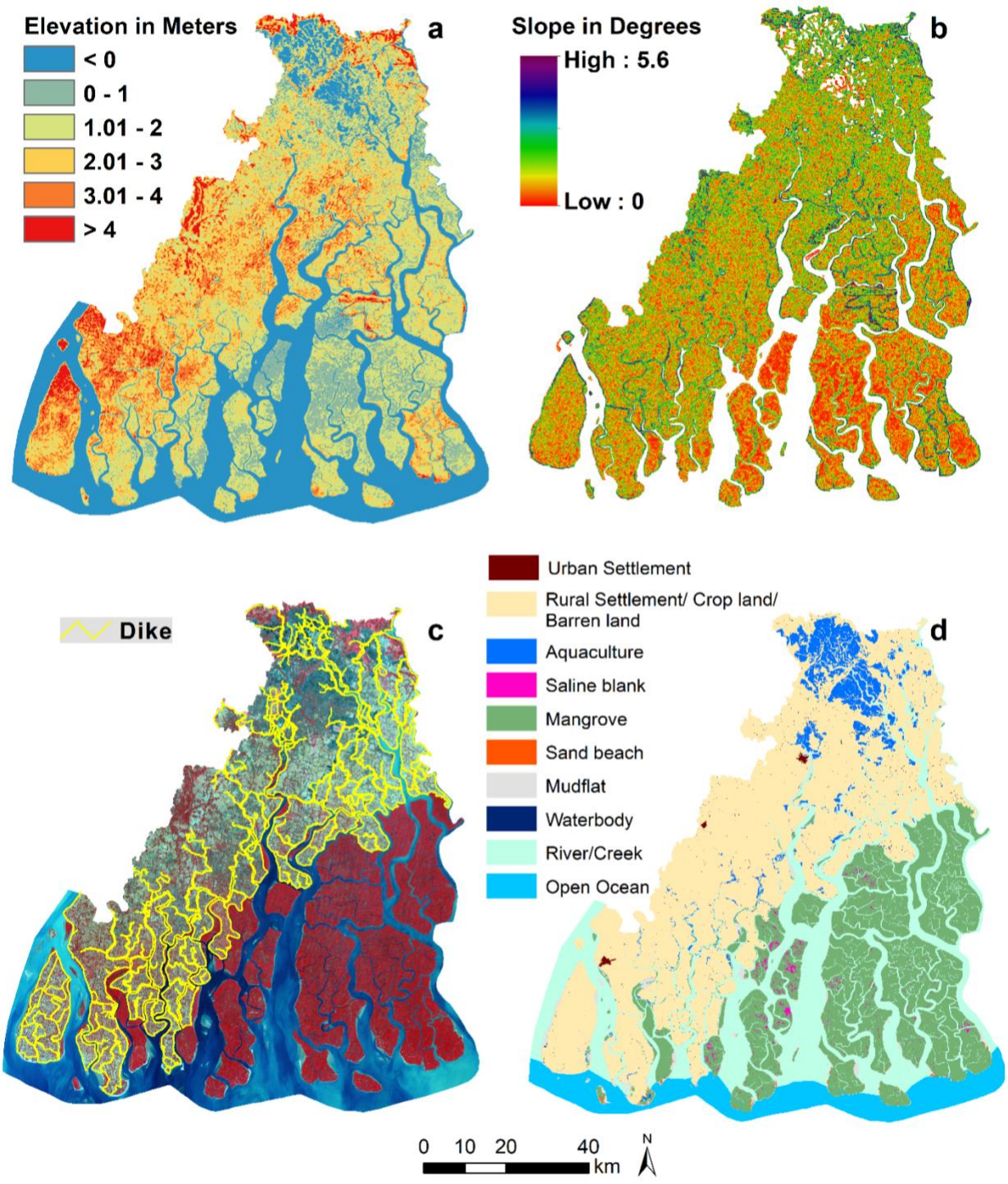

Figure 3. Principal input layers used in SLAMM simulations: a) elevation based on Coastal DEM product; b) topographic slope; c) dikes; and d) land use/land cover.

3.3 Model parameters

Tidal range varies at multiple time scales (including fortnightly spring-neap, seasonal, interannual and 18.6-year nodal tide variation) and spatially along and between the estuarine distributaries. SLAMM does not accommodate time-variation in the tidal range and tide gauges are too limited to define the spatial variation. Based on analysis of the available tidal records, a time- and space-average Great Diurnal Tidal Range (GDTR) of 3.5 m was therefore used in all simulations.

Vertical sediment accretion is an important process and there is a general consensus that tidal marshes and mangroves have some resilience to SLR such that increased inundation is at least partially compensated for by enhanced accretion (French, 2006; Woodroffe et al., 2016). Accretion, measured by sediment deposition above a surface (or near-surface marker), does not translate directly into elevation gain since it is subject to various shallow subsidence/expansion processes (Cahoon and Lynch, 1997; Krauss et al, 2014). SLAMM does not resolve this level of detail and the term accretion is used here to refer to the net elevation change resulting from sedimentation. Sediment supply to the delta from the Ganges and Brahmaputra rivers has been very large throughout the Holocene (Raff et al., 2023), although eastwards switching of the main river channels in the mid- to late-Holocene has drastically reduced direct sediment input to the western Bangladesh and Indian Sundarbans (Allison et al., 2003). Contemporary sedimentation within the Bangladesh Sundarbans has been investigated in more detail (e.g. Rogers et al., 2013), but insufficient data exist to define an empirical accretion model for the Indian Sundarban mangroves. The sparse data that do exist come mainly from multi-decadal sediment cores. Banajee et al (2012) obtained accretion rates of 3.0 to 4.8 mm yr^{-1} from ^{210}Pb-dated cores at three Sundarbans mangrove sites. These rates are broadly consistent with ^{14}C based accretion of 2.0 to 5.0 mm yr^{-1} estimated by Stanley and Hait (2000). The implication is that over the last few centuries at least, sediment supply to this part of the delta plain was sufficient for mangrove elevations to keep pace with relative SLR that was probably dominated by delta subsidence and a slow eustatic rise.

Given that higher sedimentation rates are generally localised around estuary channel margins and interior rates tend to be lower, it is reasonable to use the lower end of reported ranges (i.e. around 3.0 mm yr^{-1}) as a regional average. Modelling has demonstrated that wetland response to SLR is likely to be constrained by sediment supply (French, 2006; Kirwan et al 2010), and a

global analysis by Saintilian et al. (2020) indicates that mangroves may be unable sustain their elevations when SLR exceeds about 6 mm yr-^{1}. In the present study, we use a baseline mangrove accretion rate of 3.0 mm yr^{-1}, which is consistent with the present evidence that mangrove elevations are currently not quite keeping pace with relative SLR (Samanta et al., 2021). We also simulate a higher rate of 6.0 mm yr^{-1} to approximate the upper threshold of Saintilian et al. (2020) in the sediment-limited context of the Indian Sundarbans.

3.4 Data-driven modelling of coastal land loss due to erosion

The SLAMM 6.7 routines for fetch and depth limited wind wave erosion require too much data for application to the Sundarbans estuaries, and its prediction of open coast shoreline erosion routine based on the Bruun (1962) model in which retreat is fixed at 100 x SLR is too generic. Accordingly, a separate data-driven model was devised to predict shoreline retreat as a function of SLR. This uses the earlier results of Samanta et al. (2021), who analysed shoreline changes along the open coast and larger estuary mouth regions in relation to mean sea level variations for a series of 5-year time epochs between 1990 and 2020. Their results showed that, in the low-lying delta plain environment of the Sundarbans, SLR appears to drive much more rapid shoreline retreat (up to five times the standard Bruun approximation). By the end of 21st century, present retreat rates of up to about 38 m yr^{-1} are projected to increase to as much as 180 m yr^{-1}.

3.5 SLR scenarios

Three realistic non-linear climate-induced SLR scenarios based on IPCC (2019) (Table 1) were adopted from Nicholls et al. (2021). The high end of the likely ranges for RCP2.6 (low), RCP4.5 (moderate) and RCP8.5 (high) emission scenarios are used, giving a eustatic SLR of 0.59 m, 0.72 m and 1.1 m by 2100.

Table 1: Climate-induced eustatic SLR scenarios used in this study (derived from Nicholls et al., 2021).

	RCP2.6 (m)	RCP4.5 (m)	RCP8.5 (m)
1995	0.00	0.00	0.00
2025	0.15	0.15	0.15
2055	0.32	0.35	0.38
2085	0.50	0.59	0.82
2100	0.59	0.72	1.10

3.5 Management scenarios

Simulations were performed for two management scenarios - 'Continued Protection' and 'Managed Realignment'. Table 2 summarises all of the model runs.

In the Continued Protection scenario, it is assumed that all existing protective dikes are maintained (with any implied increases in crest elevation). This restricts the ability of mangroves to migrate inland over the inhabited areas within the Biosphere Reserve.

Under the 'Managed Realignment' scenario, it is assumed that all the existing protective dikes are removed, thereby creating additional accommodation space for the migration of mangrove inland. This would clearly affect presently inhabited areas, necessitating a relocation of people and activities.

Table 2 Summary of the model runs and the scenario assumptions. Constant subsidence of 2.5 mm yr^{-1} is assumed in all runs.

Run ID	SLR forcing scenario	Mangrove accretion rate (mm yr^{-1})	Land loss due to erosion	Management scenario
1	RCP2.6	3	included	Continued Protection
2	RCP4.5	3	included	Continued Protection
3	RCP8.5	3	included	Continued Protection
4	RCP2.6	6	included	Continued Protection
5	RCP4.5	6	included	Continued Protection
6	RCP8.5	6	included	Continued Protection
7	RCP2.6	3	included	Realignment
8	RCP4.5	3	included	Realignment
9	RCP8.5	3	included	Realignment
10	RCP2.6	6	included	Realignment
11	RCP4.5	6	included	Realignment
12	RCP8.5	6	included	Realignment

4. Results

4.1 Continued Protection scenarios

Simulated changes in habitat and land cover types for the baseline vertical mangrove accretion rate (3 mm yr^{-1}) and the assumption of continued maintenance of all existing defences are visualised in Figure 4. Little change in mangrove extent is evident in 2030, but losses become more apparent by 2050 and quite significant by 2100 as relative SLR outpaces accretion by an increasing margin, especially under RCP8.5. From Table 3, it is clear that there are some gains due to migration of mangrove but that these are always exceeded by losses such that the overall change in mangrove area is always negative. The overall net mangrove loss by 2100 ranges from about 35% under RCP2.5 to nearly 60% under RCP8.5.

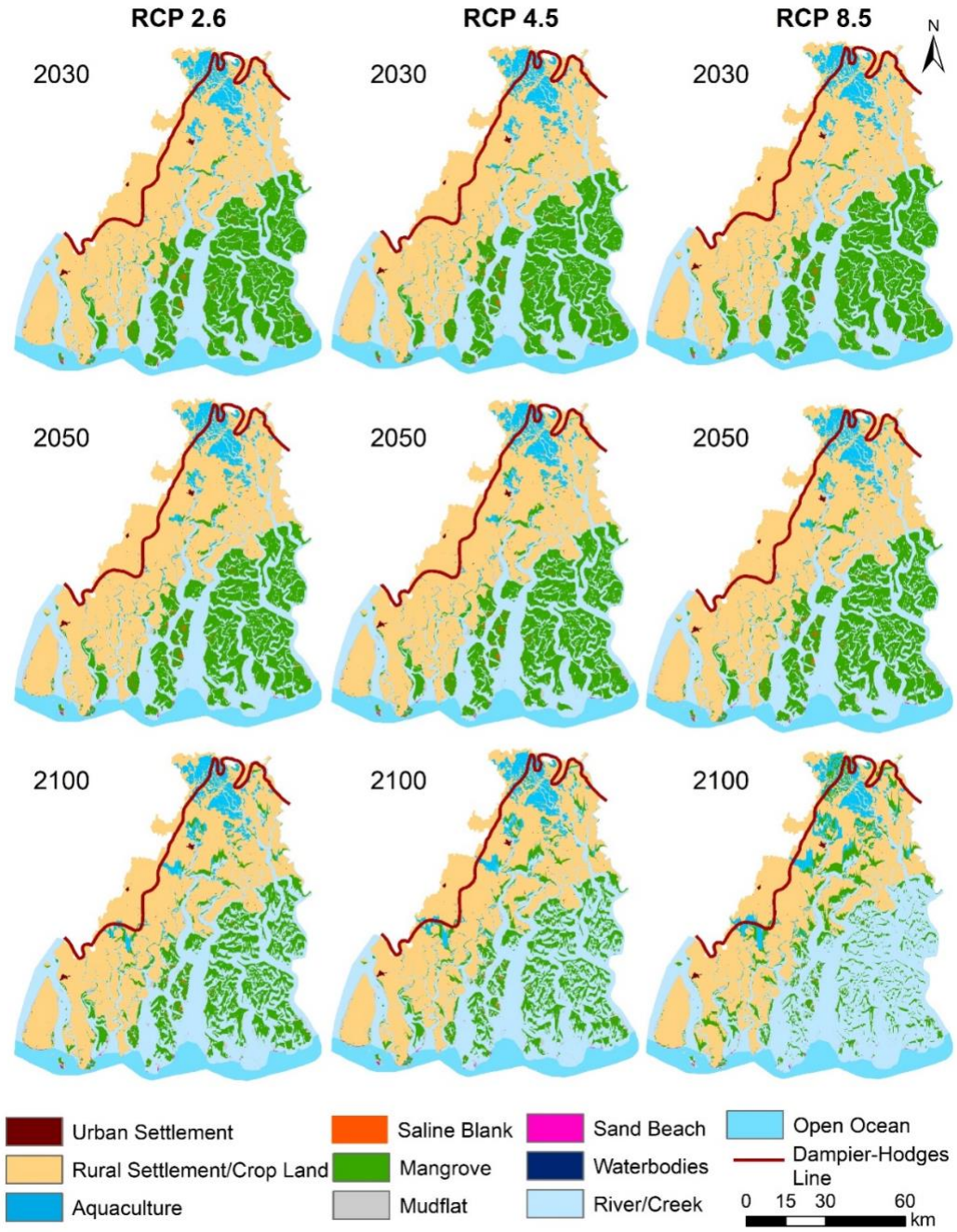

Figure 4 Simulated mangrove area changes due to the net effect of accretion and erosion for RCP2.6 (Run 1), RCP4.5 (Run 2) and RCP8.5 (Run 3) SLR scenarios using a baseline vertical mangrove accretion rate of 3 mm yr^{-1} and assuming the Continued Protection scenario.

The higher mangrove accretion rate scenario acknowledges the fact that mangroves have some resilience to SLR, provided that there is sufficient sediment supply to sustain the maintenance of their elevation at a similar level within the tidal frame. Thus, when the rate of accretion is increased to 6 mm yr^{-1}, the mangrove loss is significantly reduced (by nearly 50%) in the short-term at least under all RCP scenarios (Figure 5). Under RCP4.5 and RCP8.5, however, SLR still exceeds the capacity of accretion to maintain mangrove elevation and there is still a net loss of between 20 and 37% by 2100, respectively (Table 3).

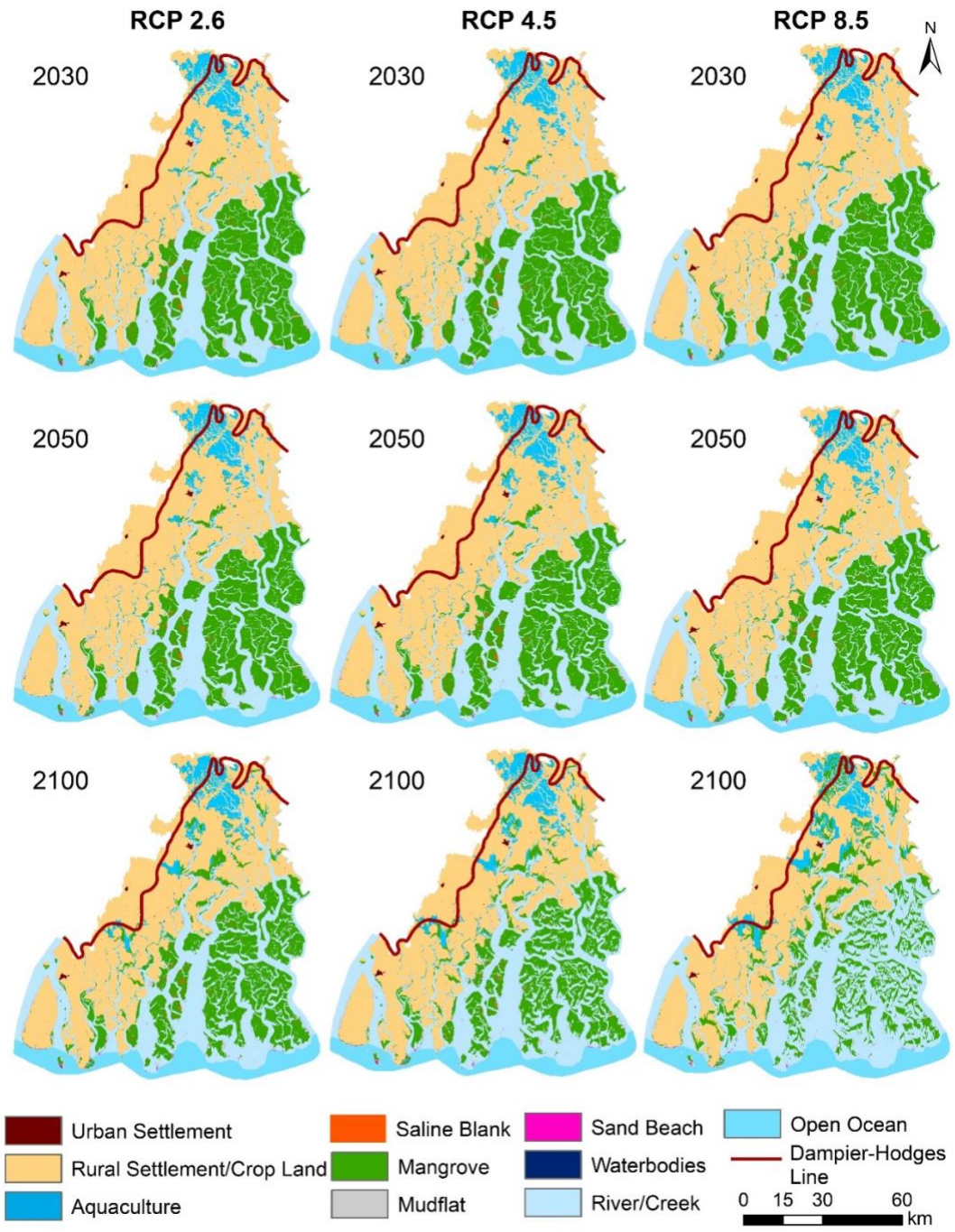

Figure 5. Simulated mangrove loss gains for RCP2.6 (Run 4), RCP4.5 (Run 5) and RCP8.5 (Run 6) scenarios, for a vertical mangrove accretion rate of 6 mm yr^{-1} to represent a plausible threshold for mangrove response to SLR, and assuming the Continued Protection scenario.

Table 3: Summary of changes in mangrove area for the combined SLAMM and empirical shoreline erosion model simulations for the various SLR, accretion and management scenarios.

Baseline vertical mangrove accretion 3 mm yr^{-1}														
Continued Protection	Run 1 RCP2.6					Run 2 RCP4.5					Run 3 RCP8.5			
	Gain (ha)	%	Loss (ha)	%		Gain (ha)	%	Loss (ha)	%		Gain (ha)	%	Loss (ha)	%
2030	1755	1	21616	10	**2030**	1801	1	22195	11	**2030**	1842	1	22759	11
2050	4534	2	38876	18	**2050**	5240	2	42202	20	**2050**	5754	3	45708	22
2100	15340	7	87823	42	**2100**	20220	10	109010	52	**2100**	44651	21	168421	80
Higher vertical mangrove accretion 6 mm yr^{-1}														
Continued Protection	Run 4 RCP2.6					Run 5 RCP4.5					Run 6 RCP8.5			
	Gain	%	Loss	%		Gain	%	Loss	%		Gain	%	Loss	%
2030	1756	1	12624	6	**2030**	1801	1	13078	6	**2030**	1843	1	13666	6
2050	4549	2	22047	10	**2050**	5343	3	24524	12	**2050**	6019	3	27236	13
2100	18291	9	45808	22	**2100**	20487	10	62942	30	**2100**	44081	21	122401	58
Baseline vertical mangrove accretion 3 mm yr^{-1}														
Managed Realignment	Run 7 RCP2.6					Run 8 RCP4.5					Run 9 RCP8.5			
	Gain	%	Loss	%		Gain	%	Loss	%		Gain	%	Loss	%
2030	19360	9	21640	10	**2030**	19858	9	22215	11	**2030**	20398	10	22782	11
2050	37683	18	38909	18	**2050**	39785	19	42239	20	**2050**	40804	19	45749	22
2100	54329	26	87992	42	**2100**	66752	32	109294	52	**2100**	113855	54	168782	80
Higher vertical mangrove accretion 6 mm yr^{-1}														
Managed Realignment	Run 10 RCP2.6					Run 11 RCP4.5					Run 12 RCP8.5			
	Gain	%	Loss	%		Gain	%	Loss	%		Gain	%	Loss	%
2030	19359	9	12624	6	**2030**	19855	9	13080	6	**2030**	20397	10	13669	6
2050	37693	18	22058	10	**2050**	40819	19	24535	12	**2050**	43921	21	27251	13
2100	85063	40	45831	22	**2100**	71729	34	63030	30	**2100**	111149	53	122707	58

4.2 Managed realignment scenarios

Under the baseline 3 mm yr^{-1} mangrove vertical accretion scenario, similarly extensive losses are projected in the outlying coastal areas, but there is significant migration and expansion of mangrove inland (Figure 6). Up to 2030, gains effectively match losses, such that net change in

mangrove area is negligible. Beyond 2050, losses start to exceed the gain through migration as extensive coastal mangrove areas cannot keep pace with SLR. Under the highest RCP8.5 SLR scenario, the mangroves effectively regain their historic limit, as approximated by the 1829-1830 Dampier Hodges line, with a net area loss of about 27% by 2100 (Table 3).

If mangrove accretion is increased to 6 mm yr^{-1} gains in area generally exceed losses. There is thus a net increase in area at all time epochs except under the RCP8.5 SLR scenario, in which a net decline in area of around 5% occurs by 2100. The change maps indicate that some areas of new mangrove forest gained by 2030 are subsequently lost by 2050 or 2100 under the RCP4.5 or RCP8.5 SLR scenarios.

These managed realignment scenarios would have significant implications for existing land-use, including a significant loss of productive land, and human occupancy within the Transition Zone (Figure 1). The implied migration would be of the order of several million people in the most extreme case. There are thus considerable socio-political barriers to the implementation of such a policy at this large scale.

4.3 Summary

The time variation in projected net gain or loss in mangrove area is summarised in Figure 8 for all 12 scenarios (Table 2). Most scenarios give rise to a net loss of mangrove by 2100. This could approach 60% of the current area under the most pessimistic combination of high SLR (i.e. RCP8.5), constrained ability of inland migration due to maintenance of all current defensive alignments, limited mangrove resilience (low vertical accretion close to present rate). Given a sufficient supply of sediment to maximise vertical accretion up to the historic limit of around 6 mm yr^{-1} suggested for this region (Saintilian et al., 2020), then losses are greatly reduced, but still remain significant (in the range 10 to 30% by 2100). Managed realignment has the effect of delaying the onset of significant loss by allowing migration inland, and if a more resilient sedimentary response is assumed then the mangrove area can actually increase. Even then, however, a net loss in mangrove area starts to become apparent by 2100 under RCP8.5 as the high rate of SLR outpaces the ability of mangroves to persist in the extensive outlying delta region.

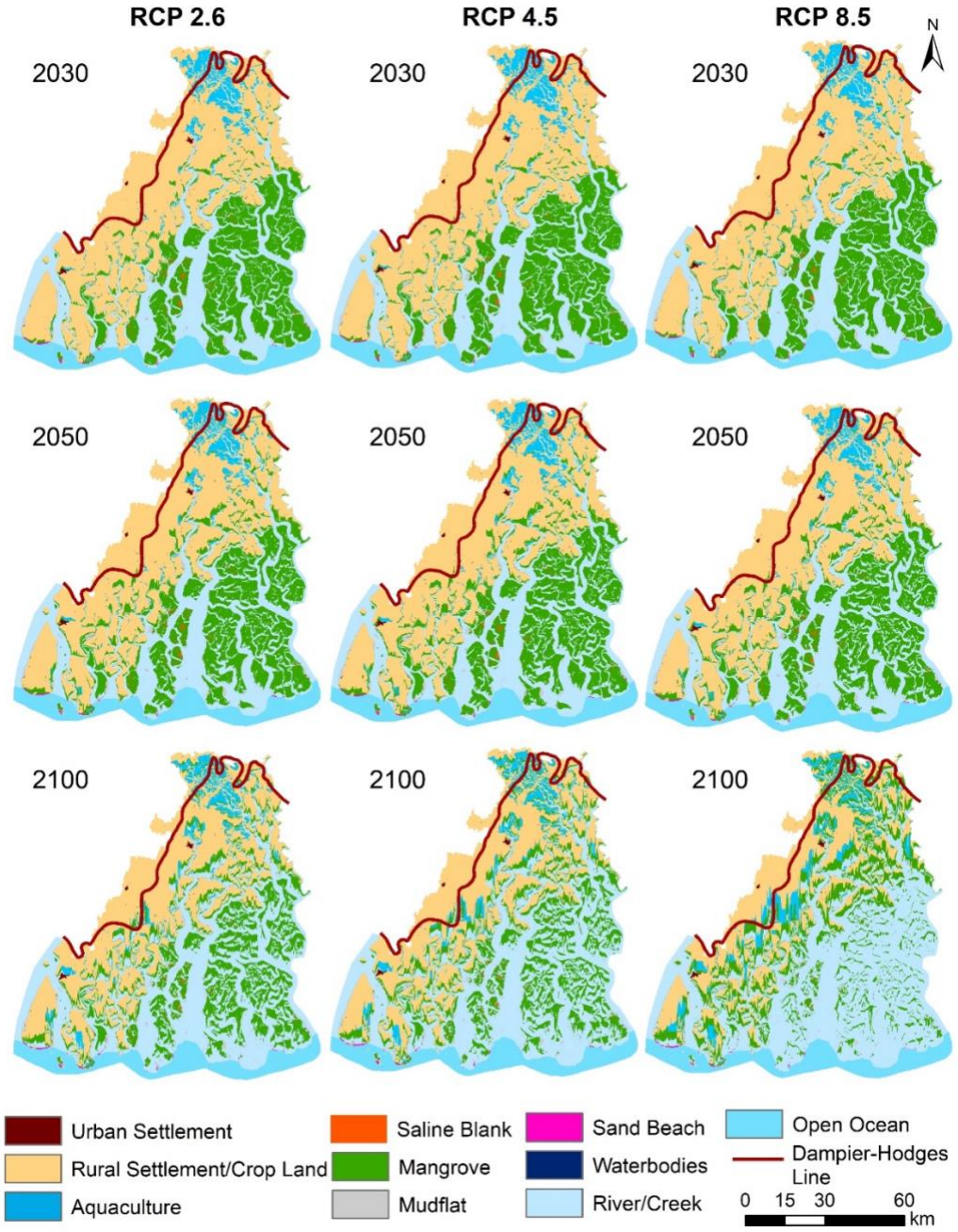

Figure 6 Simulated mangrove loss / gain for RCP2.6 (Run 7), RCP4.5 (Run 8) and RCP8.5 (Run 9) SLR scenarios using a baseline vertical mangrove accretion rate of 3 mm yr^{-1} and assuming the Managed Realignment scenario (inland migration of mangroves allowed).

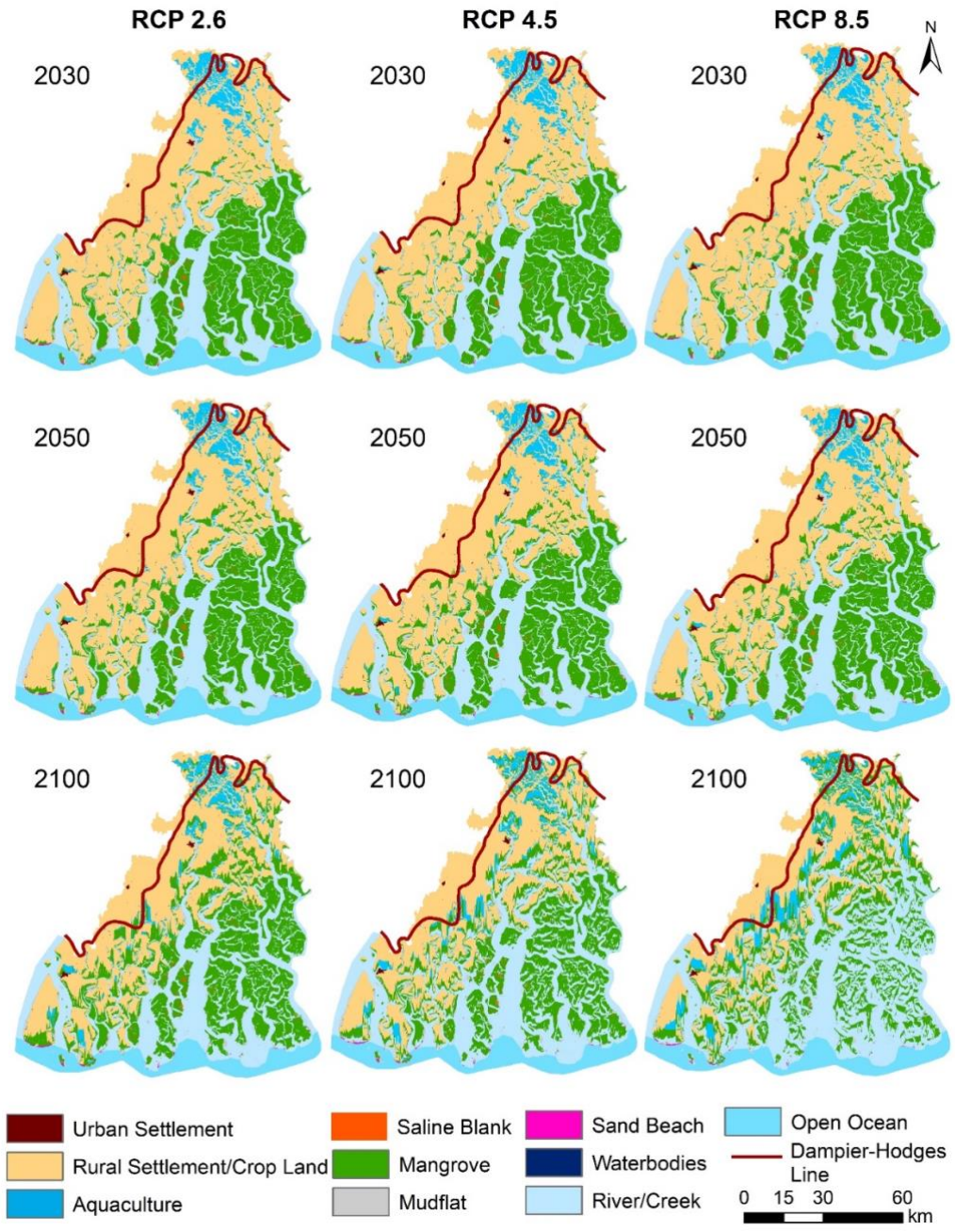

Figure 7 Simulated mangrove loss / gain for RCP2.6 (Run 10), RCP4.5 (Run 11) and RCP8.5 (Run 12) SLR scenarios using a baseline vertical accretion rate of 6 mm yr^{-1} and assuming the Managed Realignment scenario (inland migration of mangroves allowed).

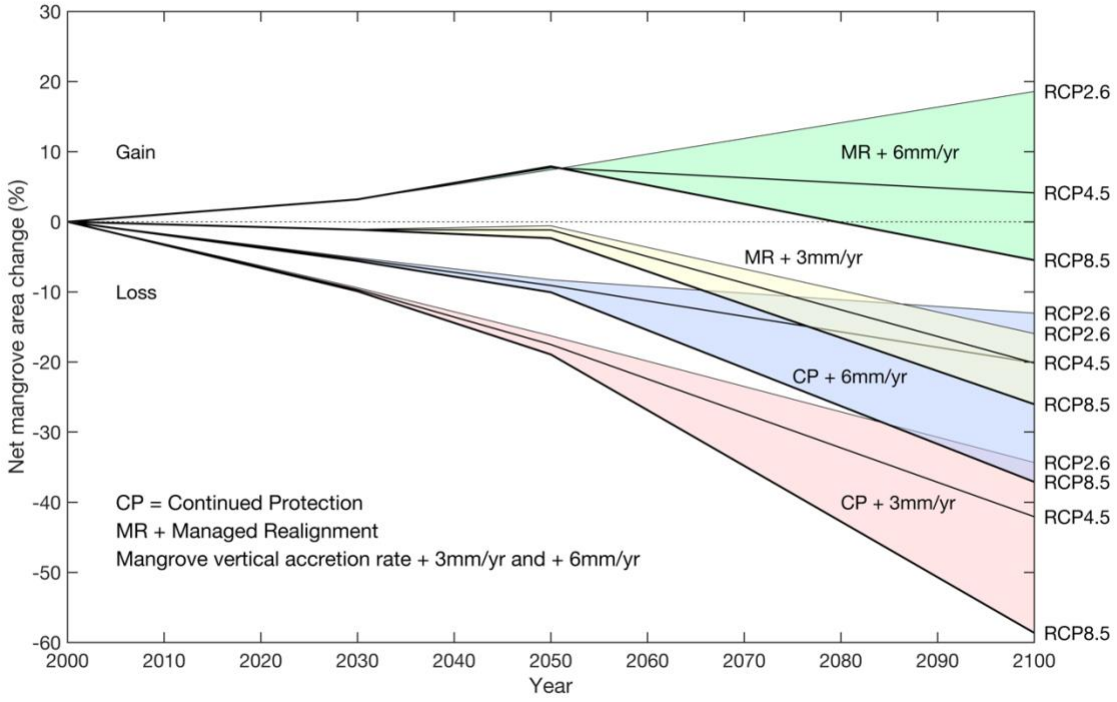

Figure 8. Summary of the projected net change in mangrove area relative to the 2000 baseline, under all of the 12 modelled SLR, mangrove accretion and management scenario combinations (Table 2).

5. Discussion

This analysis shows the benefits of model-based simulations to explore possible future pathways for the evolution of mangrove forest cover in the Indian Sundarbans. Current concerns about the implications of human-induced climate for the future of the Sundarbans have often been often framed in terms of sea-level rise. However, as recognised conceptually and in our exploratory model, there are important non-climate factors that also determine the future trajectories of the Sundarbans and a systemic understanding is required in terms of relative sea-level rise (including deltaic subsidence), sediment availability (which is linked to both climate change and river basin management; Raff et al 2023), and the availability of accommodation space (linked to coastal

defence policy). The simulations presented here provide useful insights into the relative importance of these drivers of changing mangrove area and the role of science-based management.

The model assesses the area of mangroves in the Indian Sundarbans as the main indicator. Based on observations, mangrove area has slowly declined over the last few decades (Samanta et al., 2021), and the model results suggest that this trend will continue and likely accelerate due to a combination of erosion and inundation if no new accommodation space is provided. Under most of the scenarios modelled here, there is a net decline mangrove area, with greater losses associated with higher rates of sea-level rise, lower accretion and the maintenance of the current flood defences. In the worst case, projected losses exceed 50% of the mangroves by 2100, such that the viability of the Indian Sundarbans as a habitat is called into question and its designation as a World Heritage Site could be threatened.

Large-scale managed realignment of the existing flood defences has the potential to create new accommodation space and greatly reduce the loss of mangroves and possibly even lead to an expansion in overall mangrove area under the most favourable scenarios. However, the societal consequences of this policy are significant as land-use transitions will mean that large numbers of people will need to be relocated. A summary of the changes in land use is provided in Table S1 (Supplementary Materials). The changes are similar between the two different mangrove accretion scenarios, despite the very different outcomes in terms of mangrove area presented in the preceding section; this is because a given land use can ultimately transition either to mangrove or to open water depending on the accretion scenario. Depending on the climate scenario, between 14 and 28 % of agricultural and rural land use and 13 to 34% of the area currently used for aquaculture are projected to be lost by 2100. Population projections and simulated numbers of people to be relocated, based on the predicted land-use changes, are summarised in Table S2 (Supplementary Materials). Realistic projections of future population extend only to 2050, but even at this point, nearly 650,000 people are affected. These projections represent a minimum, based on the cumulative cell transitions within the SLAMM simulations. In reality, the viability of isolated land-use units would be questionable and the likely relocation of population required would be larger. A more complete de-population of the affected area would also be more consistent with the maintenance of the current World Heritage status of the Sundarbans.

It is important to place these findings within the context of the strong regional demographic pressure from Kolkata, which had a population of 11 million in 1990, 14.7 million in 2018 and has a projected population of 17.6 million by 2030 (UN DESA, 2018). As a result, there is a strong conflict between rising sea levels in the Sundarbans and increasing land values and human needs to the north. Implementation of managed realignment as a general policy across the region would likely be politically difficult to implement, at least in the next few decades. As a result, continued and potentially accelerated decline of the Sundarbans and its mangroves appears to be the most likely scenario for the future in the absence of any other radical interventions in the system (cf. Sanchez-Arcilla et al., 2022).

In policy terms, strong support for climate mitigation (to reduce sea-level rise), better understanding and enhancement of sediment supply and accretion (to understand and promote vertical resilience) and promotion of managed realignment where possible (to increase accommodation space) should all be encouraged. These measures need to be combined with more systematic monitoring of mangrove change and improved understanding of the processes driving these changes.

In the short-term at least, direct intervention to reduce loss of mangrove due to shoreline erosion (e.g. Chowdhury et al., 2019) could buy time in which to implement the more challenging management responses referred to above. It is unrealistic to hold the present shorelines over the whole of the 21st century. The effect of halting shoreline erosion completely was simulated by de-activating the erosion sub-model. This showed that, with no erosion, between 95 and 125 km^2 of mangrove loss (equivalent to 4.5% to 6.0% of the initial baseline area) could be avoided by 2050 depending on the climate and accretion scenario used (for full inundation-only simulation results see Table S3 in Supplementary Materials). Erosion accounts for a larger proportion of small absolute mangrove area losses in 2030 but diminishes in importance in later time epochs and under higher SLR scenarios. Enhanced mangrove accretion reduces losses due to inundation, such that the relative importance of shoreline erosion increases (see Table S4 in Supplementary Materials). In situ protection against inundation might also be considered to sustain the mangroves, but is more questionable as a feasible response. For example, the building of defences around marshes in the Mississippi delta actually accelerated their losses due to a combination of reductions in sediment input and water logging (Boesch et al., 1994). The currently preferred policy is to

increase freshwater and sediment fluxes to enhance marsh resilience (Day et al., 2007; 2019) and it can be argued that the same broad approaches are appropriate for the Sundarbans (cf. Rahman et al., 2022). Various studies have noted that the sediment fluxes from the Ganges-Brahmaputra rivers are declining (Rahman et al., 2018; Dunn et al., 2019) and that this is likely to continue under the influence of planned damming and diversion schemes (Higgins et al., 2018). While these sediment fluxes do not feed directly into the Indian Sundarbans, their decline will diminish regional sediment availability within the northern Bay of Bengal as a whole, which is clearly detrimental to the achievement of the higher vertical mangrove accretion rates modelled in the present study. A mass-balance analysis presented by Raff et al (2023) highlights the inherent robustness of the whole sediment system given the very large potential fluvial supply that might actually be enhanced with changing monsoon precipitation. On the other hand, their analysis also shows that large sediment deficits emerge at higher rates of SLR and in scenarios that continue to envisage large-scale river damming and diversion (e.g. Dunn et al., 2018). This is broadly consistent with our imposition of a constraint to vertical sediment accretion, which leads to significant simulated losses in mangrove area end of the 21st century. It must be emphasised that SLAMM is a purely kinematic model, based on the net effect of various influences on the elevation of a given habitat cell, and that it does include any direct computation of sediment mass balance; better models directly constrained by sediment supply are needed to properly integrate understanding of mangrove and delta dynamics.

Given that sediment supply is clearly a major factor determining mangrove resilience, other interventions at the coast may be of limited effectiveness. Measures to “protect” or “adapt” the mangroves in situ remain largely experimental in nature and any extension of their use would need to be carefully tested and monitored in terms of their costs, benefits and effectiveness (cf. Sanchez-Arcilla et al., 2022).

Based on the results here, a decline in mangrove area remains likely with long-term adverse consequences for the ecosystem services and biodiversity supported by the SBR. More understanding of the determinants of the viability of the mangroves as a habitat would be useful to fully evaluate the implications of the current decline and the existence of any key tipping points. In particular, is not clear when the critical habitat requirements for indicator species such as the Bengal Tiger will fail to be met and what management targets are desirable.

Taking these issues forward in science-based management is constrained by the limited range of calibrated models and the data on which these depend. Modelling of coastal wetland ecosystem dynamics is crucially dependent upon the availability of sufficiently accurate topographic data. Satellite DEMs are still the only source of topographic data for this region and we have evaluated the best available products in this paper. More accurate DEMs would better constrain the outputs from the kind of model that we have employed and are essential to allow the development of better, more physically-based models. Hence, a key goal should be high-resolution airborne Lidar coverage of the entire Sundarbans region, supported by routine change analysis building on Samanta et al (2021). Limited field observations restrict the parameterisation of the mangrove accretion model. Another priority should be field investigations at enough locations to develop accretion models that are constrained not only by inundation regime but also by sediment supply (Lovelock et al., 2015). All of this implies further development of the systems approach that has been utilised in this analysis, including a detailed exploration of the sediment budget and its controlling factors. The efforts in this regard for coastal restoration of the Mississippi delta (Day et al 2019) provide a useful model that might be adapted to the Sundarbans.

6. Conclusions

This paper has presented new exploratory simulations of possible changes in the area of mangrove forest within the Indian Sundarbans up to the year 2100. The widely used Sea Level Affecting Marshes Model (SLAMM) has been coupled with a separate empirical shoreline erosion model to simulate a range of sea-level rise (combining climate change and geological subsidence), mangrove accretion and management scenarios. Not unexpectedly, sea-level rise emerges as a strong driver of mangrove loss, although mangroves have greater resilience if sediment supply is assumed to be sufficient to allow vertical accretion at the maximum rate of 6 mm yr^{-1} inferred from previous studies. The natural migration of mangrove inland is checked by the widespread flood defences that are currently in place, such that all scenarios project net overall loss of between 10 and 60 % by 2100.

System-wide managed realignment of current flood defences would allow migration of mangroves, although only the less pessimistic sea-level rise and higher mangrove vertical accretion scenarios give rise to a net gain in mangrove until the end of the century. Moreover, such a

management response would necessitate significant re-location of human population and associated economic activities and would undoubtedly prove politically challenging to implement in practise.

CRediT authorship contribution statement

Sugata Hazra and Robert Nicholls identified the research problem and conceptualized the study, with Jon French. Sourav Samanta set up the SLAMM modelling platform and performed the analysis with the guidance of all the other authors. Partho Mondal conducted the elevation analysis and MSL conversion. All the authors contributed to the manuscript, with Sourav Samanta preparing the maps and figures and Jon French finalising the manuscript.

Declaration of competing interest

We declare that we have no conflict of interest.

Acknowledgement

This research was funded under the "Towards a Sustainable Earth: Environment-human systems and the UN Global Goals" (TaSE) program in the project "Opportunities and trade-offs between the SDGs for food, welfare and the environment in deltas". Funding was provided by NERC Grant NE/S012478/1, Formas Grant 2019-00045, and the UKIERI-DBT (Grant BT/IN/TaSE/70/SH/2018-19) under UK-India Education Research Initiative. RN has been supported by funding from the European Union's Horizon 2020 research and innovation program under grant agreement no. 101037097 (REST-COAST project).

References

Akumu, C.E., Pathirana, S., Baban, S., Bucher, D., 2011. Examining the potential impacts of sea level rise on coastal wetlands in north-eastern NSW, Australia. J. Coast. Conserv. 15, 15-22. doi.org/10.1007/s11852-010-0114-3

Ali, S.A., Khatun, R., Ahmad, A., Ahmad, S.N., 2020. Assessment of cyclone vulnerability, hazard evaluation and mitigation capacity for analyzing cyclone risk using GIS technique: a study on Sundarban biosphere reserve, India. Earth Syst. Environ. 4(1), 71-92. https://doi.org/10.1007/s41748-019-00140-x

Allison, M.A., Khan, S.R., Goodbred Jr, S.L., Kuehl, S.A., 2003. Stratigraphic evolution of the late Holocene Ganges–Brahmaputra lower delta plain. Sediment. Geol. 155(3-4), 317-342.

Alongi, D.M., 2008. Mangrove forests: resilience, protection from tsunamis, and responses to global climate change. Estuar. Coast. Shelf Sci. 76, 1-13.

Banerjee, K., Senthilkumar, B., Purvaja, R., Ramesh, R., 2012. Sedimentation and trace metal distribution in selected locations of Sundarbans mangroves and Hooghly estuary, Northeast coast of India. Environ. Geochem. Health 34, 27-42. https://doi.org/10.1007/s10653-011-9388-0

Barbier, E.B., Hacker, S.D., Kennedy, C., Koch, E.W., Stier, A.C., Silliman, B.R., 2011. The value of estuarine and coastal ecosystem services. Ecol. Monogr. 81(2), 169-193. https://doi.org/10.1890/10-1510.1

Barik, J.; Chowdhury, S., 2014. True mangrove species of Sundarbans delta, West Bengal, eastern India. Check List 10(2), 329-34. https://doi.org/10.15560/10.2.329

Barik, J., Mukhopadhyay, A., Ghosh, T., Mukhopadhyay, S.K., Chowdhury, S.M., Hazra, S., 2018. Mangrove species distribution and water salinity: an indicator species approach to Sundarban. J. Coast. Conserv. 22(2), 361-368. https://doi.org/10.1007/s11852-017-0584-7

Boesch, D., Josselyn, M.N., Mehta, A.J., Morris, J.T, Nuttle, W.J., Simenstad , C.A., Swift, D.J.P., 1994. Scientific assessment of coastal wetland loss, restoration and management in Louisiana. J. Coast. Res., Special Issue 20, 109pp.

Brown, S., Nicholls, R.J., 2015. Subsidence and human influences in mega deltas: the case of the Ganges–Brahmaputra–Meghna. Sci. Tot. Environ. 527, 362-374. https://doi.org/10.1016/j.scitotenv.2015.04.124

Bruun, P. 1962. Sea level rise as a cause of shore erosion. Amer. Soc. Civil Eng., Proc. J. Waterw. Harb. Div. 88, 117-130.

Cahoon, D.R., Lynch, J.C., 1997. Vertical accretion and shallow subsidence in a mangrove forest of southwestern Florida, U.S.A.. Mangroves & Salt Marshes 1, 173-186. https://doi.org/10.1023/A:1009904816246

Carugati, L., Gatto, B., Rastelli, E., Martire, M.L., Coral, C., Greco, S., Danovaro, R., 2018. Impact of mangrove forests degradation on biodiversity and ecosystem functioning. Sci. Rep. 8(1), 1-11.

Chowdhury, M.S.N., Walles, B., Sharifuzzaman, S., Hossain, M.S., Ysebaert, T., Smaal, A.C., 2019. Oyster breakwater reefs promote adjacent mudflat stability and salt marsh growth in a monsoon dominated subtropical coast. Sci. Rep. 9, 8549. https://doi.org/10.1038/s41598-019-44925-6

Clough, J., Polaczyk, A., Propato, M., 2016. Modeling the potential effects of sea-level rise on the coast of New York: Integrating mechanistic accretion and stochastic uncertainty. Environ. Model. Softw. 84, 349-362. https://doi.org/10.1016/j.envsoft.2016.06.023

Cole Ekberg, M.L., Raposa, K.B., Ferguson, W.S., Ruddock, K., Burke, E., 2017. Development and application of a method to identify salt marsh vulnerability to sea level rise. Estuar. Coasts 40, 694-710. doi.org/10.1007/s12237-017-0219-0

Costanza, R., Sklar, F.H., White, M.L., 1990. Modeling coastal landscape dynamics. BioScience 40, 91-107.

Craft, C., Clough, J., Ehman, J., Joye, S., Park, R., Pennings, S., Guo, H., Machmuller, M., 2009. Forecasting the effects of accelerated sea-level rise on tidal marsh ecosystem services. Frontiers Ecol. Environ. 7(2), 73-78.

Day, J.W., Boeasch, D.F., Clairain, E.J., Kemp, G.P., Laska, S.B. Mitsch, W.J., Orth, K., Mashiriqui, H., Reed, D.J., Shabman, L., Simenstad, C.A., Steerver, B.J., Twilley, R.R., Watson, C.C., Wells, J.T., Whigham, D.F., 2007. Restoration of the Mississippi Delta: Lessons from Hurricanes Katrina and Rita. Science, 315, 1679-1684. https://www.science.org/doi/10.1126/science.1137030

Day, J.W., Colten, C., Kemp, G.P., 2019. Chapter 10 - Mississippi Delta restoration and protection: shifting baselines, diminishing resilience, and growing nonsustainability. In: Wolanski, E., Day, J.W., Elliott, M., Ramachandran, R. (Eds.) Coasts and Estuaries. Elsevier, pp. 167-186. https://www.sciencedirect.com/science/article/abs/pii/B9780128140031000101?via%3Dihub

Dunn, F.E., Nicholls, R.J., Darby, S.E., Cohen, S., Zarfl, C., Fekete, B.M., 2018. Projections of historical and 21st century fluvial sediment delivery to the Ganges-Brahmaputra-Meghna, Mahanadi, and Volta deltas. Sci. Total Environ. 642, 105–116. https://doi.org/10.1016/j.scitotenv.2018.06.006

Dunn, F.E., Darby, S.E., Nicholls, R.J., Cohen, S., Zarfl, C., Fekete, B.M., 2019. Projections of declining fluvial sediment delivery to major deltas worldwide in response to climate change and anthropogenic stress. Environ. Res. Lett. 14, 084034. https://iopscience.iop.org/article/10.1088/1748-9326/ab304e/meta

Farr, T.G., Rosen, P.A., Caro, E., Crippen, R., Duren, R., Hensley, S., Kobrick, M., Paller, M., Rodriguez, E., Roth, L., Seal, D., 2007. The shuttle radar topography mission. Rev. Geophys. 45(2). https://doi.org/10.1029/2005RG000183

French, J.R., 2006. Tidal marsh sediment trapping efficiency and resilience to environmental change: exploratory modelling of tidal, sea-level and sediment supply forcing in predominantly allochthonous systems. Mar. Geol. 235, 119-36.

Ghosh, A., Schmidt, S., Fickert, T., Nüsser, M., 2015. The Indian Sundarban mangrove forests: history, utilization, conservation strategies and local perception. Diversity 7(2), 149-169.

Gilman, E., Van Lavieren, H., Ellison, J., Jungblut, V., Wilson, L., Areki, F., Brighouse, G., Bungitak, J., Dus, E., Henry, M., Kilman, M., 2006. Pacific Island Mangroves in a Changing Climate and Rising Sea. UNEP Regional Seas Reports and Studies No. 179.

Giri, C., Pengra, G., Zhu, Z., Singh, A., Larry, L., Tieszen, L.L., 2007. Monitoring mangrove forest dynamics of the Sundarbans in Bangladesh and India using multi-temporal satellite data from 1973 to 2000. Estuar. Coast. Shelf Sci. 73, 91-100, https://doi.org/10.1016/j.ecss.2006.12.019

Hazra, S., Ghosh, T., DasGupta, R., Sen, G., 2002. Sea level and associated changes in the Sundarbans. Sci. Cult. 68(9-12), 309–321.

Higgins, S.A., Overeem, I., Rogers, K.G., Kalina, E.A., 2018. River linking in India: Downstream impacts on water discharge and suspended sediment transport to deltas. Elementa 6, 20. https://doi.org/10.1525/elementa.269

Huq, S., Ali, S.I., Rahman, A.A., 1995. Sea-level rise and Bangladesh: A preliminary analysis. J. Coast. Res. Special Issue 14. Potential impacts of accelerated sea-level rise on developing countries, 44-53.

IPCC 2019. Special Report on the Ocean and Cryosphere in a Changing Climate. Intergovernmental Panel on Climate Change (IPCC). https://www.ipcc.ch/srocc/home/ Accessed December 6, 2021.

Kirwan, M.L., Guntenspergen, G.R., D'Alpaos, A.D., Morris, J.T., Mudd, S.M., Temmerman, S., 2010. Limits on the adaptability of coastal marshes to rising sea level. Geophys. Res. Lett. 37 L23401.

Krauss, K.W., McKee, K.L., Lovelock, C.E., Cahoon, D.R., Saintilian, N., Reef, R., Chen, L., 2014. How mangrove forests adjust to rising sea level. New Phytol. 202, 19–34. https://doi.org/10.1111/nph.12605

Kulp, S.A., Strauss, B.H., 2018. CoastalDEM: a global coastal digital elevation model improved from SRTM using a neural network. Rem. Sens. Environ. 206, 231-239.

Li, S., Meng, X., Ge, Z. and Zhang, L., 2015. Evaluation of the threat from sea-level rise to the mangrove ecosystems in Tieshangang Bay, southern China. Ocean & Coast. Manage. 109, 1-8.

Loucks, C., Barber-Meyer, S., Hossain, M.A.A., Barlow, A., Chowdhury, R.M., 2010. Sea level rise and tigers: predicted impacts to Bangladesh's Sundarbans mangroves. Climatic Change 98, 291. https://doi.org/10.1007/s10584-009-9761-5

Lovelock, C., Cahoon, D., Friess, D., Guntenspergen, G.R., Krauss, K.W., Reef, R., Rogers, K., Saunders, M.L., Sidik, F., Swales, A., Saintilan, N., Thuyen, L.H., Triet, T., 2015. The vulnerability of Indo-Pacific mangrove forests to sea-level rise. Nature 526, 559–563. https://doi.org/10.1038/nature15538

Marcinko, C.L., Nicholls, R.J., Daw, T.M., Hazra, S., Hutton, C.W., Hill, C.T., Clarke, D., Harfoot, A., Basu, O., Das, I., Giri, S., 2021. The development of a framework for the integrated assessment of SDG trade-offs in the Sundarban biosphere reserve. Water 13(4), 528.

McLeod, E., Poulter, B., Hinkel, J., Reyes, E., Salm, R., 2010. Sea-level rise impact models and environmental conservation: A review of models and their applications. Ocean & Coast. Manage. 53(9), 507-517.

Menéndez, P., Losada, I.J., Torres-Ortega, S. et al. 2020. The global flood protection benefits of mangroves. Sci. Rep. 10, 4404. https://doi.org/10.1038/s41598-020-61136-6

Mukul, S.A., Alamgir, M., Sohel, M.S.I., Pert, P.L., Herbohn, J., Turton, S.M., Khan, M.S.I., Munim, S.A., Reza, A.H.M.A, Laurance, W.F. 2019. Combined effects of climate change and sea-level rise project dramatic habitat loss of the globally endangered Bengal tiger in the Bangladesh Sundarbans. Sci. Tot. Environ. 663, 830-840. https://doi.org/10.1016/j.scitotenv.2019.01.383

Nicholls, R.J., Cazenave, A., 2010. Sea-level rise and its impact on coastal zones. Science 328(5985), 1517-1520. https://doi.org/10.1126/science.1185782

Nicholls, R.J., Hanson, S.E., Lowe, J.A., Slangen, A.B.A., Wahl, T., Hinkel, J., Long, A., 2021. Integrating new sea-level scenarios into coastal risk and adaptation assessments: An ongoing process. Wiley Interdiscip. Rev. Clim. Change 12 (3), https://doi.org/10.1002/wcc.706

Padhy, S.R., Bhattacharyya, P., Dash, P.K., Reddy, C.S., Chakraborty, A., Pathak, H., 2020. Seasonal fluctuation in three mode of greenhouse gases emission in relation to soil labile carbon pools in degraded mangrove, Sundarban, India. Sci. Tot. Environ. 705, 135909. https://doi.org/10.1016/j.scitotenv.2019.135909

Payo, A., Mukhopadhyay, A., Hazra, S. et al. 2016. Projected changes in area of the Sundarban mangrove forest in Bangladesh due to SLR by 2100. Clim. Change 139, 279–291. https://doi.org/10.1007/s10584-016-1769-z

Pitchaikani, J.S., 2020. Vertical current structure in a macro-tidal, well mixed Sundarban ecosystem, India. J. Coast Conserv. 24(5), 1–11. https://doi.org/10.1007/s11852-020-00782-4

Prado, P., Alcaraz, C., Benito, X., Caiola, N., Ibanez, C., 2019. Pristine vs. human-altered Ebro Delta habitats display contrasting resilience to RSLR. Sci. Tot. Environ. 655, 1376-1386. https://doi.org/10.1016/j.scitotenv.2018.11.318

Raff, J.S., Goodbred Jr., S.L., Pickering, J.L., Sincavage, R.S., Ayers, J.C. Hossain, M.S., Wilson, C.A., Paola, C., Steckler, M.S., Mondal, D.R., Grimaud, J-L., Grall, C.J., Rogers, K.G., Ahmed, K.M., Akhter, S.H., Carlson, B.N., Chamberlain, E.L., Dejter, M., Gilligan, J.M, Hale, R.P., Khan, M.R., Muktadir, M.G., Rahman, M.R., Williams, L.A., 2023. Sediment delivery to sustain the Ganges- Brahmaputra delta under climate change and anthropogenic impacts. Nat. Comm. 14, 2429. https://doi.org/10.1038/s41467-023-38057-9

Rahman, M.M., Haque, A., Nicholls, R.J., Darby, S.E., Urmi, M.T., Dustegir, M.M., Dunn, F.E., Tahsin, A., Razzaque, S., Horsburgh, K., Haque, M.A., 2022. Sustainability of the coastal zone of the Ganges-Brahmaputra-Meghna delta under climatic and anthropogenic stresses. Sci. Tot. Environ. 829, 154547. https://doi.org/10.1016/j.scitotenv.2022.154547

Reyes, E., White, M. L., Martin, J. F., Kemp, G. P., Day, J. W., Aravamuthan, V. 2000. Landscape modeling of coastal habitat change in the Mississippi Delta. Ecology 81(8), 2331–2349. https://doi.org/10.2307/177118

Rizzoli, P., Martone, M., Gonzalez, C., Wecklich, C., Tridon, D.B., Bräutigam, B., Bachmann, M., Schulze, D., Fritz, T., Huber, M., Wessel, B., 2017. Generation and performance assessment of the global TanDEM-X digital elevation model. ISPRS J. Photogram. Rem. Sens. 132, 119-139.

Rogers, K.G., Goodbred Jr., S.L., Mondal, D.R., 2013. Monsoon sedimentation on the 'abandoned' tide-influenced Ganges-Brahmaputra delta plain. Estuar. Coast. Shelf Sci. 131, 297-309. http://dx.doi.org/10.1016/j.ecss.2013.07.014

Samanta, S., Hazra, S., Mondal, P.P., Chanda, A., Giri, S., French, J.R., Nicholls, R.J., 2021. Assessment and Attribution of Mangrove Forest Changes in the Indian Sundarbans from 2000 to 2020. Rem. Sens. 13(24), 4957. https://doi.org/10.3390/rs13244957

Saintilian, N., Khan, N.S., Ashe, E., Kelleway, J.J., Rogers, K., Woodroffe, C.D., Horton, B.P., 2020. Thresholds of mangrove survival under rapid sea level rise. Science 368, 1118-1121.

Sanchez-Arcilla, A. et al. 2022. Barriers and enablers for upscaling coastal restoration. Nature-Based Solutions (in press)

Sarker, S., Reeve, R., Thompson, J., Paul, N.K., Matthiopoulos, J., 2016. Are we failing to protect threatened mangroves in the Sundarbans world heritage ecosystem? Sci. Rep. 6, 21234. https://doi.org/10.1038/srep21234

Schuerch, M., Spencer, T., Temmerman, S., Kirwan, M.L., Wolff, C., Lincke, D., McOwen, C.J., Pickering, M.D., Reef, R., Vaefeidis, A.T., Hinkel, J., Nicholls, R.J., Brown, S. 2018. Future response of global coastal wetlands to sea-level rise. Nature 561(7722), 231-234.

Spencer, T., Schuerch, M., Nicholls, R.J., Hinkel, J., Lincke, D., Vafeidis, A.T., Reef, R., McFadden, L. and Brown, S., 2016. Global coastal wetland change under sea-level rise and related stresses: The DIVA wetland change model. Glob. Planet. Change 139, 15-30. https://doi.org/10.1016/j.gloplacha.2015.12.018

Sriyanie, M., 2008. Mangroves. Coastal ecosystems series, Volume 2. Mangroves. Colombo, IUCN, 28pp.

Stanley, D.J., Hait, A.K., 2000. Holocene depositional patterns, neotectonics and Sundarban mangroves in the western Ganges-Brahmaputra delta. J. Coast. Res. 26-39.

Tabak, N.M., Laba, M., Spector, S., 2016. Simulating the effects of sea level rise on the resilience and migration of tidal wetlands along the Hudson River. PLoS ONE 11(4): e0152437. https://doi.org/10.1371/journal.pone.0152437

United Nations Department of Economic and Social Affairs, 2018. World Urbanization Prospects 2018. United Nations, New York. https://population.un.org/wup/publications/Files/WUP2018-Highlights.pdf

Warren Pinnacle Consulting Inc, 2016. SLAMM 6.7 Technical Documentation. Sea Level Affecting Marshes Model.

White, J.R., DeLaune, R.D., Justic, D., Day, J.W., Pahl, J., Lane, R.R., Boynton, W.R., Twilley, R.R., 2019. Consequences of Mississippi River diversions on nutrient dynamics of coastal wetland soils and estuarine sediments: A review. Estuar. Coast. Shelf Sci. 224, 209-216. https://doi.org/10.1016/j.ecss.2019.04.027

Woodroffe, C.D., Rogers, K., McKee, K.L., Lovelock, C.E., Mendelssohn, I.A., Saintilan, N., 2016. Mangrove sedimentation and response to relative sea-level rise. Ann. Rev. Mar. Sci. 8, 243-266. https://doi.org/10.1146/annurev-marine-122414-034025

Wu, W., Yeager, K.M., Peterson, M.S., Fulford, R.S., 2015. Neutral models as a way to evaluate the Sea Level Affecting Marshes Model (SLAMM). Ecol. Model. 303, 55-69.

Supplementary Materials

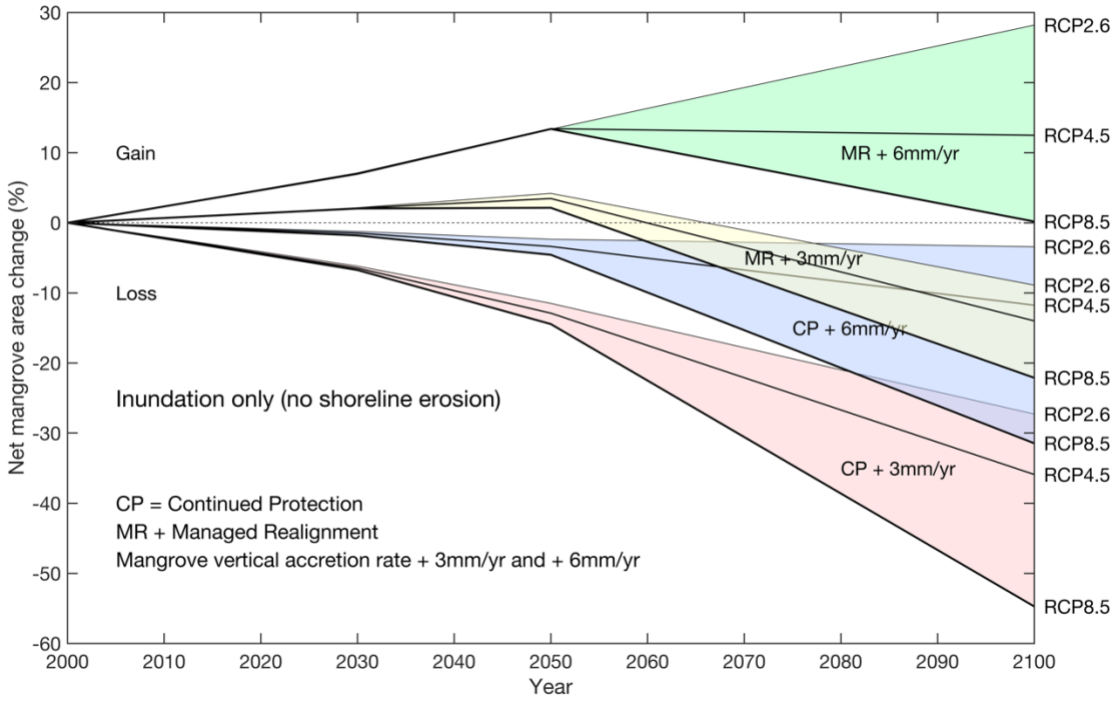

Figure S1. Projected net change in mangrove area relative to the 2000 baseline, under all of the 12 modelled SLR, mangrove accretion and management scenarios with the shoreline erosion model de-activated – i.e. changes due only to inundation (compare with Figure 8 in main paper).

Table S1 Land use transitions and the % of each land cover type lost under each of the modelled managed realignment (MR) scenarios. Note that the initial transitions are to mangrove, but mangrove cells may become open water if mangrove cannot subsequently keep pace with rising sea level or is lost through shoreline erosion.

MR (no dike) scenario with 3 mm/yr vertical mangrove accretion		
RCP2.6	**2030**	
	Area converted (ha)	**% lost**
agriculture/rural/barren to mangrove	19,223	5.2
aquaculture to mangrove	136	0.4
	2050	
agriculture/rural/barren to mangrove	36,676	10.0
aquaculture to mangrove	997	2.8
saline blank to mangrove	10	0.4
	2100	
agriculture/rural/barren to mangrove	49,382	13.5
aquaculture to mangrove	4,676	13.3
saline blank to mangrove	271	11.5
RCP4.5	**2030**	
Conversion	**Area converted (ha)**	**% lost**
agriculture/rural/barren to mangrove	19,700	5.4
aquaculture to mangrove	158	0.5
	2050	
agriculture/rural/barren to mangrove	38,608	10.5
aquaculture to mangrove	1,163	3.3
saline blank to mangrove	15	0.6
	2100	
agriculture/rural/barren to mangrove	59,928	16.3
aquaculture to mangrove	6,482	18.5
saline blank to mangrove	343	14.6
RCP 8.5	**2030**	
Conversion	**Area converted (ha)**	**% lost**
agriculture/rural/barren to mangrove	20,163	5.5
aquaculture to mangrove	235	0.7
	2050	
agriculture/rural/barren to mangrove	39,349	10.7
aquaculture to mangrove	1,415	4.0
saline blank to mangrove	40	1.7
	2100	
agriculture/rural/barren to mangrove	101,237	27.6
aquaculture to mangrove	11,782	33.6
saline blank to mangrove	837	35.6

MR (no dike) scenario with 6 mm/yr vertical mangrove accretion		
RCP2.6	**2030**	
Conversion	**Area converted (ha)**	**% lost**
agriculture/rural/barren to mangrove	19,222	5.2
aquaculture to mangrove	136	0.4
	2050	
agriculture/rural/barren to mangrove	36,687	10.0
aquaculture to mangrove	997	2.8
saline blank to mangrove	10	0.4
	2100	
agriculture/rural/barren to mangrove	80,274	21.9
aquaculture to mangrove	4,652	13.3
saline blank to mangrove	137	5.8
RCP4.5	**2030**	
Conversion	**Area converted (ha)**	**% lost**
agriculture/rural/barren to mangrove	19,696	5.4
aquaculture to mangrove	158	0.5
	2050	
agriculture/rural/barren to mangrove	39,645	10.8
aquaculture to mangrove	1,162	3.3
saline blank to mangrove	12	0.5
	2100	
agriculture/rural/barren to mangrove	64,984	17.7
aquaculture to mangrove	6,467	18.5
saline blank to mangrove	278	11.8
RCP 8.5	**2030**	
Conversion	**Area converted (ha)**	**% lost**
agriculture/rural/barren to mangrove	20,162	5.5
aquaculture to mangrove	235	0.7
	2050	
agriculture/rural/barren to mangrove	42,468	11.6
aquaculture to mangrove	1,416	4.0
saline blank to mangrove	37	1.6
	2100	
agriculture/rural/barren to mangrove	98,519	26.8
aquaculture to mangrove	11,784	33.6
saline blank to mangrove	846	36.0

Table S2 Projected population for Community Development Blocks for 2031 and 2051, and the number of people for whom relocation would be required based upon the simulated land-use transitions for each of the climate scenarios (RCP2.6, RCP4.5 and RCP8.5).

		Population requiring relocation				Population requiring relocation		
Block name	**2031 population**	**RCP 2.6**	**RCP4.5**	**RCP 8.5**	**2051 population**	**RCP 2.6**	**RCP4.5**	**RCP 8.5**
Basanti	472,488	32,346	32,994	33,801	634,287	82,760	89,598	95,275
Canning I	460,213	8,807	9,181	9,496	662,762	26,051	28,100	30,139
Canning II	402,307	1,054	1,054	1,068	600,987	8,130	13,225	14,137
Gosaba	298,554	27,339	27,884	28,497	356,382	59,223	63,245	67,544
Haroa	279,530	930	1,075	1,191	346,487	5,186	7,013	7,967
Hasnabad	252,749	6,324	6,545	6,754	299,576	15,930	17,809	20,647
Hingalganj	222,943	15,088	15,458	15,782	287,485	36,561	39,232	42,043
Jaynagar- I	381,999				541,815			
Jaynagar II	371,829	11,114	11,415	11,750	536,330	29,852	32,095	34,120
Kakdwip	347,434	15,387	15,737	16,005	386,501	31,062	33,180	37,185
Kultali	339,756	20,334	20,716	21,166	488,559	55,470	59,582	63,541
Mathurapur I	279,088				393,840	855	1,202	1,555
Mathurapur II	257,732	19,566	20,087	20,673	283,661	40,200	43,167	45,940
Minakhan	254,867	578	618	815	304,710	6,246	7,826	8,673
Namkhana	215,026	10,766	11,105	11,500	230,942	26,170	29,779	31,769
Patharpratima	420,589	21,509	22,148	22,547	511,899	50,723	55,019	58,681
Sagar	249,676	9,660	10,063	10,405	267,119	22,498	25,562	27,564
Sandeshkhali I	224,599	5,768	5,990	6,838	300,941	18,118	20,927	24,736
Sandeshkhali II	231,997	11,039	11,345	11,608	331,958	30,059	32,988	35,826
Total	**5,963,376**	**217,608**	**223,415**	**229,895**	**7,766,241**	**545,096**	**599,550**	**647,340**

Table S3. Summary of changes in mangrove area for the combined SLAMM and empirical shoreline erosion model simulations for the various SLR, accretion and management scenarios, with the shoreline erosion model de-activated – i.e. changes due only to inundation (compare with Table 3 in main paper).

Baseline vertical mangrove accretion 3 mm yr^{-1}														
Continued Protection	Run 1 RCP2.6					Run 2 RCP4.5					Run 3 RCP8.5			
	Gain (ha)	%	Loss (ha)	%		Gain (ha)	%	Loss (ha)	%		Gain (ha)	%	Loss (ha)	%
2030	1755	1	14805	7	**2030**	1801	1	15453	7	**2030**	1842	1	16077	8
2050	4534	2	28805	14	**2050**	5240	2	32458	15	**2050**	5754	3	36255	17
2100	15340	7	72940	35	**2100**	20220	10	96021	45	**2100**	44651	21	160219	76
Higher vertical mangrove accretion 6 mm yr^{-1}														
Continued Protection	Run 4 RCP2.6					Run 5 RCP4.5					Run 6 RCP8.5			
	Gain	%	Loss	%		Gain	%	Loss	%		Gain	%	Loss	%
2030	1756	1	4382	2	**2030**	1801	1	4929	2	**2030**	1843	1	5653	3
2050	4549	2	9523	5	**2050**	5343	3	12474	6	**2050**	6019	3	15660	7
2100	18291	9	25530	12	**2100**	20487	10	45315	21	**2100**	44081	21	110524	52
Baseline vertical mangrove accretion 3 mm yr^{-1}														
Managed Realignment	Run 7 RCP2.6					Run 8 RCP4.5					Run 9 RCP8.5			
	Gain	%	Loss	%		Gain	%	Loss	%		Gain	%	Loss	%
2030	19360	9	14829	7	**2030**	19858	9	15473	7	**2030**	20398	10	16100	8
2050	37683	18	28839	14	**2050**	39785	19	32495	15	**2050**	40804	19	36295	17
2100	54329	26	73109	35	**2100**	66752	32	96305	46	**2100**	113855	54	160580	76
Higher vertical mangrove accretion 6 mm yr^{-1}														
Managed Realignment	Run 10 RCP2.6					Run 11 RCP4.5					Run 12 RCP8.5			
	Gain	%	Loss	%		Gain	%	Loss	%		Gain	%	Loss	%
2030	19359	9	4382	2	**2030**	19855	9	4931	2	**2030**	20397	10	5655	3
2050	37693	18	9534	5	**2050**	40819	19	12485	6	**2050**	43921	21	15675	7
2100	85063	40	25553	12	**2100**	71729	34	45403	22	**2100**	111149	53	110830	53

Table S4 Proportion of the simulated mangrove loss attributed to shoreline erosion for each of the hybrid SLAMM + empirical erosion model runs. Erosion accounts for a larger proportion of small absolute mangrove area losses in 2030 but diminishes in importance in later time epochs and under higher SLR scenarios. Enhanced mangrove accretion reduces losses due to inundation, such that the relative importance of shoreline erosion increases.

		% mangrove loss due to shoreline erosion			
		2030	2050	2100	
CP + 3 mm/yr accretion	Run 1	31.5	25.9	16.9	RCP2.6
	Run 2	32.6	23.1	11.9	RCP4.5
	Run 3	29.4	20.7	4.9	RCP8.5
CP + 6 mm/yr accretion	Run 4	65.3	56.8	44.3	RCP2.6
	Run 5	62.3	49.1	28.0	RCP4.5
	Run 6	58.6	42.5	9.7	RCP8.5
MR + 3 mm/yr accretion	Run 7	31.5	25.9	16.9	RCP2.6
	Run 8	30.3	23.1	12.4	RCP4.5
	Run 9	29.3	20.7	4.9	RCP8.5
MR + 6 mm/yr accretion	Run 10	65.3	56.8	44.2	RCP2.6
	Run 11	62.3	49.1	28.0	RCP4.5
	Run 12	58.6	42.5	9.7	RCP8.5